

See discussions, stats, and author profiles for this publication at: <https://www.researchgate.net/publication/10684755>

# The Myristoylated Amino Terminus of G $\alpha$ i 1 Plays a Critical Role in the Structure and Function of G $\alpha$ i 1 Subunits in Solution

ARTICLE *in* BIOCHEMISTRY · AUGUST 2003

Impact Factor: 3.02 · DOI: 10.1021/bi0345438 · Source: PubMed

---

CITATIONS

24

---

READS

125

6 AUTHORS, INCLUDING:



[Anita M Preininger](#)

Aquinas College Nashville

29 PUBLICATIONS 1,156 CITATIONS

SEE PROFILE



[Heidi E Hamm](#)

Vanderbilt University

224 PUBLICATIONS 13,447 CITATIONS

SEE PROFILE

# The Myristoylated Amino Terminus of $G\alpha_{i1}$ Plays a Critical Role in the Structure and Function of $G\alpha_{i1}$ Subunits in Solution

Anita M. Preininger,<sup>‡</sup> Ned Van Eps,<sup>§</sup> Nan-Jun Yu,<sup>§</sup> Martina Medkova,<sup>‡</sup> Wayne L. Hubbell,<sup>§</sup> and Heidi E. Hamm<sup>\*,||</sup>

*Institute for Neuroscience, Department of Molecular Pharmacology and Biological Chemistry, Northwestern University, Chicago, Illinois 60611, Department of Pharmacology, Vanderbilt University Medical Center, Nashville, Tennessee 37232-6600, and Departments of Ophthalmology and Chemistry, University of California, Los Angeles, California 90095*

Received April 7, 2003; Revised Manuscript Received May 11, 2003

**ABSTRACT:** To determine the role of the myristoylated amino terminus of  $G\alpha$  in G protein activation, nine individual cysteine mutations along the myristoylated amino terminus of  $G\alpha_i$  were expressed in a functionally Cys-less background. Thiol reactive EPR and fluorescent probes were attached to each site as local reporters of mobility and conformational changes upon activation of  $G\alpha_iGDP$  by  $AlF_4^-$ , as well as binding to  $G\beta\gamma$ . EPR and steady state fluorescence anisotropy are consistent with a high degree of immobility for labeled residues in solution all along the amino terminus of myristoylated  $G\alpha_i$ . This is in contrast to the high mobility of this region in nonmyristoylated  $G\alpha_i$  [Medkova, M., et al. (2002) *Biochemistry* 41, 9962–9972]. Steady state fluorescence measurements revealed pronounced increases in fluorescence upon activation for residues 14–17 and 21 located midway through the 30-amino acid stretch comprising the amino-terminal region. Collectively, the data suggest that myristoylation is an important structural determinant of the amino terminus of  $G\alpha_i$  proteins.

Agonist-bound seven-transmembrane receptors bind to and activate heterotrimeric  $G$  proteins, resulting in dissociation of  $G\alpha^1$  and  $G\beta\gamma$  subunits. These subunits can activate a myriad of effectors such as adenylyl cyclases, phosphodiesterases, phospholipases, and ion channels. Crystal structures of G proteins and their subunits in various activation states describe in detail regions of conformational flexibility, called switch regions. In addition to changes in switch regions, solution studies have revealed conformational changes occurring in the carboxy terminus of G proteins upon activation (1). In the amino terminus, few structural details are available in the absence of  $G\beta\gamma$ , because this region is missing or disordered in  $G\alpha_iGDP$  (2),  $G\alpha_iGTP\gamma S$ , and  $G\alpha_iGTP\gamma S$  (3, 4) crystal structures. Although the  $G\alpha_iGDP$  structure shows ordered residues in the amino and carboxy termini folded

into a compact microdomain (5), the relevance of this microdomain is obscured by the presence of phosphate ion-mediated interactions and crystal contacts.

Functional studies reveal that amino-terminal regions of  $G\alpha$  proteins can impact G protein activity. For example, phosphorylation of the amino terminus of  $G\alpha_z$  potentiates signaling by preventing binding of  $G\beta\gamma$  and GAPs (6). Graf et al. showed that removal of 18 amino-terminal residues from  $G\alpha_i$  reduces the affinity for  $G\beta\gamma$  and reduces the extent of  $GTP\gamma S$  binding (7), suggesting the amino terminus contributes to the conformation of  $G\alpha$  subunits involved in nucleotide binding and  $G\beta\gamma$  association. Heterotrimeric G protein structures (8, 9) reveal the amino terminus of  $G\alpha$  as a clearly resolved  $\alpha$ -helix in contact with  $G\beta\gamma$ , comprising a portion of the binding interface between  $G\alpha$  and  $G\beta\gamma$  subunits. Since G protein cycling requires dissociation and reassociation of  $G\alpha$  and  $G\beta\gamma$  subunits, the amino terminus of  $G\alpha$  may be directly or indirectly involved in signaling by mediating changes in affinity between these subunits.

In nature, all  $G\alpha_i$  subunits are myristoylated and, with the exception of  $G\alpha_o$ , reversibly palmitoylated. A stable amide bond irreversibly links myristate to the amino-terminal glycine in  $G\alpha_o$  and  $G\alpha_i$  family members  $G\alpha_{i1}$ – $G\alpha_{i3}$ ,  $G\alpha_z$ , and  $G\alpha_q$ ; all but  $G\alpha_i$  are also palmitoylated, as are  $G\alpha_s$  and  $G\alpha_q$  (10). Because all crystallized G proteins to date are without lipid modifications (as they tend to hinder crystal formation), little is known about the role of the myristate in G protein structure and signaling. Biochemical studies have demonstrated that myristoylation of the amino terminus results in a 10-fold increase in  $G\alpha$ – $G\beta\gamma$  binding affinity (11, 12). Efficient ADP ribosylation on the carboxy terminus of  $G\alpha$ , commonly used as a measure of  $G_{i/o}$  heterotrimeric integrity (13), occurs preferentially with myristoylated  $G\alpha$  subunits (14). This could be due to a reduced level of

\* To whom correspondence should be addressed. E-mail: heidi.hamm@vanderbilt.edu.

<sup>‡</sup> Northwestern University.

<sup>§</sup> University of California.

<sup>||</sup> Vanderbilt University Medical Center.

<sup>1</sup> Abbreviations:  $G_t$ , G protein of the rod outer segment, transducin;  $G_i$ , family of G proteins coupled to inhibition of adenylyl cyclase;  $G\alpha$ ,  $\alpha$ -subunits of various G proteins;  $G\beta\gamma$ ,  $\beta\gamma$ -subunit of G proteins; ROS, rod outer segment; myr, myristoylated; SDS, sodium dodecyl sulfate; EDTA, ethylenedinitrilotetraacetic acid; PMSF, phenylmethanesulfonyl fluoride; DTT, dithiothreitol; MES, 2-(N-morpholino)ethanesulfonic acid; LY, lucifer yellow vinyl sulfone, dipotassium salt; SDSL, site-directed spin labeling; EPR, electron paramagnetic resonance; M8, 2-(4'-maleimidylanilino)naphthalene-6-sulfonic acid, sodium salt; R1, S-(1-oxy-2,2,5,5-tetramethylpyrrolidine-3-methyl)methanethiosulfonate;  $GTP\gamma S$ , guanosine 5'-O-(3-thiotriphosphate); GDP, guanosine 5'-diphosphate; GTP, guanosine 5'-triphosphate; ADP, adenosine 5'-diphosphate; Tris, tris(hydroxymethyl)aminomethane; IPTG, isopropyl  $\beta$ -D-thiogalactoside; GFC, gel filtration chromatography; FRET, fluorescence resonance energy transfer; ARF1, ADP ribosylation factor 1; MARCKS, myristoylated alanine-rich C kinase substrate; PKA, cAMP-dependent protein kinase.

heterotrimer formation in the absence of myristate. Additionally, myristoylation of the amino terminus may stabilize the carboxy-terminal conformation needed for efficient ribosylation. These results suggest a role for myristoylation in the structure and function of  $G\alpha$  subunits.

Myristoylation and concomitant increases in hydrophobicity of  $G\alpha$  subunits may influence their localization, but the extent of this relationship is unclear. Inhibition of myristoylation does not abrogate membrane association of  $G\alpha_i$  in COS cells (15). Galbiati et al. (15) also found myristoylation alone is insufficient to anchor  $G\alpha_{i1}$  proteins to membranes. A more recent study suggests palmitate levels regulate the movement of myristoylated  $G\alpha_i$  into lipid rafts involved in the spatial regulation of G protein signaling (16). Similarly, a myristoylation and palmitoylation deficient mutant of  $G\alpha_i$  cannot be localized to membranes unless palmitoylation is restored (17). Furthermore, creation of a receptor- $G\alpha_i$  fusion protein restores receptor-mediated signaling to a membrane binding deficient nonpalmitoylated  $G\alpha_{i1}$  (18). It is possible that relative levels of palmitate and myristate modulate localization of  $G\alpha$  subunits, but the reversible nature of palmitoylation makes it a more likely regulator of membrane binding than myristoylation (19). Confounding the issue, the farnesyl group of  $G\gamma$  is involved in the cooperative binding of acylated  $G\alpha$  subunits to membranes (20).

A role for myristoylation, beyond membrane binding, is controversial. Myristoylation may play a role in protein-protein interactions, and may be required for palmitoyl acyl transferase to recognize and palmitoylate cysteines in the amino terminus of  $G\alpha$  proteins. One study found impaired palmitoylation in a nonmyristoylated  $G\alpha_o$  mutant which was capable of binding to membranes and  $G\beta\gamma$  subunits (21), while another study found that myristoylation was not needed for palmitoylation (15). Myristoylation has also been implicated in effector activation. A constitutively active  $G\alpha_{i2}$  requires myristoylation to effectively inhibit adenylyl cyclase in COS cells (22). Likewise, a membrane-localized nonmyristoylated  $G\alpha_i$  mutant was shown to be defective in inhibition of adenylyl cyclase (22), supporting a role for myristoylation in effector activation.

A previous paper characterized the environment of nonmyristoylated amino-terminal  $G\alpha_i$  residues in a series of fluorescence and EPR experiments. To gain insight into the role of myristoylation in the structure and function of  $G\alpha_i$  subunits, EPR and fluorescence studies have now been conducted using myristoylated  $G\alpha_i$  proteins. EPR provides quantitative data on side chain and backbone dynamics, while fluorescence provides data on the polarity of the environment and fluorophore mobility. In the myristoylated  $G\alpha_i$  cysteine mutants,  $AlF_4^-$  activation caused pronounced increases in the fluorescence of several amino-terminal residues (14–17 and 21), similar to the somewhat smaller increases seen for LY-labeled residues in nonmyristoylated  $G\alpha_i$  proteins. Compared to the highly mobile, random coil seen in nonmyristoylated  $G\alpha_i$ GDP proteins, EPR and fluorescence anisotropy of myristoylated  $G\alpha_i$ GDP proteins demonstrated very little mobility for labeled  $G\alpha$  residues in the GDP-bound state. Taken together, these results reveal pronounced differences in the activation and  $G\beta\gamma$  binding of myristoylated  $G\alpha_i$  proteins in solution compared to those of their nonmyristoylated counterparts, and a significant role for myristoylation in  $G\alpha$  amino-terminal structure.

## MATERIALS AND METHODS

**Materials.** Guanosine 5'-diphosphate (GDP) was purchased from Boehringer Mannheim (Indianapolis, IN). Lucifer yellow vinyl sulfone (LY) was purchased from Sigma (St. Louis, MO), and MAINS (M8), 2-(4'-maleimidylanilino)-naphthalene-6-sulfonic acid, sodium salt, was purchased from Molecular Probes (Eugene, OR). The sulfhydryl spin-label reagent *S*-(1-oxy-2,2,5,5-tetramethylpyrrolidine-3-methyl)-methanethiosulfonate (R1) was a generous gift of K. Hideg (University of Pecs, Pecs, Hungary). All other reagents and chemicals were of the highest available purity.

**Preparation of  $G\beta\gamma$  and Holotransducin.** Native holotransducin and  $G\beta\gamma$  subunits were prepared as previously described (23). Purified proteins were stored at  $-20^\circ\text{C}$  in a buffer containing 10 mM Tris (pH 7.5), 100 mM NaCl, 5 mM  $\beta$ -mercaptoethanol, and 40% glycerol.  $G\beta\gamma$  was further purified by gel filtration chromatography in a buffer containing 10 mM Tris (pH 7.5) and 100 mM NaCl prior to being used in fluorescence and EPR experiments.

**Construction, expression, and purification of the mutant  $G\alpha$  protein** was conducted as described previously (24), with minor modifications that led to myristoylated proteins. Briefly, an expression vector with various single cysteine-substituted residues in the amino terminus was cotransfected into BL21(DE3) GOLD cells (Stratagene, La Jolla, CA) with plasmid pbb131 encoding *N*-myristoyl transferase for protein expression (11). The *N*-myristoyl transferase vector was generously provided by M. Linder (Washington University, St. Louis, MO), as was the parent  $G\alpha_{i1}$ . The parent  $G\alpha_{i1}$  vector contains a hexahistidine tag between amino acid residues M119 and T120 of the  $G\alpha_{i1}$  coding region. To be able to specifically label the  $G\alpha$  subunit at the desired cysteine-substituted residues, six solvent-exposed native cysteines of  $G\alpha_{i1}$  had been previously removed to produce the hexa mutant  $G\alpha_{i1}$ -C3S/C66A/C214S/C305S/C325A/C351I (Hexa I) prior to introduction of single cysteine mutations along the amino terminus (25) which are expressed as myristoylated proteins in the study presented here. The parent  $G\alpha_i$  Hexa I protein behaves in a manner similar to that of the wild type in functional assays, including intrinsic  $\text{Trp}^{211}$  activation, receptor-mediated GTP $\gamma$ S binding, and GTP hydrolysis in both the presence and absence of RGS4 (25). Previous mutagenesis with the QuickChange mutagenesis kit (Stratagene) resulted in the following  $G\alpha_i$  Hexa I constructs: A3C, K10C, V13C, E14C, R15C, S16C, K17C, R21C, and K29C (25). In this study, the proteins were expressed as myristoylated proteins by coexpression with the pbb131 plasmid encoding myristoyl transferase, designated  $G\alpha_i$  Hexa I CM. The individual mutant proteins are designated, for example, as Hexa I-K10CM, where CM stands for the myristoylated Cys mutant and K10 identifies the native residue (Lys) and the sequence position at residue 10. In this study, Hexa I-K10CM, Hexa I-V13CM, Hexa I-E14CM, Hexa I-R15CM, Hexa I-S16CM, Hexa I-K17CM, Hexa I-R21CM, and Hexa I-K29CM were prepared.

Expression and purification were conducted as described previously (24, 25) with minor modifications. Briefly, *Escherichia coli* cells were grown to an  $\text{OD}_{600}$  of 0.3 unit in the presence of 100  $\mu\text{g/mL}$  ampicillin and 50  $\mu\text{g/mL}$  kanamycin, and protein expression was then induced with 30  $\mu\text{M}$  IPTG at room temperature for 12–16 h. Postinduction

cells from a 1 L culture were resuspended in buffer A [50 mM NaH<sub>2</sub>PO<sub>4</sub> (pH 8) and 300 mM NaCl] containing 5 mM imidazole and leupeptin, pepstatin, and aprotinin (1  $\mu$ g/mL each) and then disrupted by sonication. The cytosolic fraction was incubated with 5 mL of a 50% slurry of Ni-NTA agarose resin (Qiagen, Valencia, CA) for 60 min at 4 °C and loaded onto an empty column. The unbound proteins were removed by washing the mixture first with 20 mL, and then 10 mL, of buffer A containing 5 mM imidazole, and 10 mM imidazole, respectively. G $\alpha$  mutant proteins were eluted with 5–10 mL of buffer A containing 40 mM imidazole. Eluted proteins were buffer exchanged against buffer B containing 50 mM Tris (pH 8), 50 mM NaCl, 1 mM MgCl<sub>2</sub>, 20% glycerol, and 20  $\mu$ M GDP and then loaded onto a 1 mL MonoQ column (Pharmacia Amersham, Piscataway, NJ). The sample was chromatographed at 700 psi on a Beckman System Gold HPLC system (Beckman Coulter, Fullerton, CA) with a linear gradient from 50 to 200 mM NaCl in buffer B, and the G $\alpha_i$  subunit was eluted at approximately 150 mM NaCl. After anion exchange had been carried out, purification resulted in greater than 85% pure myristoylated G $\alpha_i$  Hexa I proteins as estimated by Coomassie blue staining of SDS-polyacrylamide gels. Protein concentrations were determined by the Coomassie blue method (26) using bovine serum albumin as a standard (Pierce, Rockford, IL).

**Fluorescent Labeling of Proteins.** All proteins were exchanged into labeling buffer prior to modification. LY labeling of G $\alpha$  proteins was performed as described previously (25). Briefly, LY (10 mM) was added in a 5:1 molar ratio to G $\alpha$  proteins in 50 mM Tris-HCl (pH 8.0), 50 mM NaCl, 1 mM MgCl<sub>2</sub>, and 50  $\mu$ M GDP; the mixture was incubated at 4 °C for 1 h and the reaction quenched by 5 mM  $\beta$ -mercaptoethanol. G $\beta\gamma$  was labeled with fluorescent probe M8 (27) by incubation of a 10-fold molar excess of M8 with holotransducin, G $\alpha$ GDP-G $\beta_1\gamma_1$ , at 4 °C before quenching with 5 mM  $\beta$ -mercaptoethanol. Gel filtration chromatography buffer B was supplemented with AlF<sub>4</sub><sup>-</sup> (10 mM NaF and 50  $\mu$ M AlCl<sub>3</sub>) to allow recovery of unbound G $\beta\gamma$ -M8 in late fractions from chromatography on an SW2000 column (Tosoh Haas, Montgomeryville, PA). This resulted in G $\beta\gamma$ -M8 being labeled at sites distinct from the  $\alpha$ - $\beta\gamma$  binding interface. Myr-G $\alpha$ -LY proteins were purified in a similar manner by gel filtration chromatography in buffer B. The stoichiometry of labeling was calculated as a molar ratio of the concentration of fluorophore to the concentration of the labeled protein. The concentration of fluorophore was determined by measuring the absorbance of the labeled protein (430 nm for LY and 317 nm for M8) with extinction coefficients of 12 400 and 27 000 M<sup>-1</sup> cm<sup>-1</sup> for LY and M8, respectively. The protein concentration of labeled samples was determined by the Coomassie blue binding method (26) using bovine serum albumin as a standard (Pierce). The stoichiometry of labeled proteins was between 0.4 and 0.6 mol/mol for myr-G $\alpha$ -LY and markedly higher for G $\beta\gamma$ -M8, which has five cysteines available for labeling (27).

**SDS-PAGE.** Myr-G $\alpha_i$  Hexa I-LY mutant proteins were electrophoresed on a 10 to 20% Tris-glycine gel in the presence of  $\beta$ -mercaptoethanol and SDS. Illumination by UV light, followed by Coomassie staining, was used to visualize the LY-labeled proteins. To resolve myristoylated from nonmyristoylated subunits, 1 M urea was added to running

buffer and samples were prepared as described above and electrophoresed on a 10% Tris-glycine gel at 100 V for 180 min, resulting in a mobility shift for the myristoylated proteins as compared to nonmyristoylated protein (11, 28).

**Spectrofluorometric Assays.** To monitor the ability of labeled G $\alpha_i$  mutants to undergo activation, intrinsic tryptophan (Trp<sup>211</sup>) fluorescence (29) of the labeled proteins (100 nM) was monitored in buffer B by excitation at 280 nm and emission at 340 nm before and after the addition of AlF<sub>4</sub><sup>-</sup> (10 mM NaF and 50  $\mu$ M AlCl<sub>3</sub>) using an AMINCO Bowman Series 2 luminescence spectrometer.

Activation and G $\beta\gamma$ -dependent changes in amino-terminal residues were measured in buffer B using excitation at 430 nm and emission at 520 nm before and after the addition of AlF<sub>4</sub><sup>-</sup> or the G $\beta\gamma$  subunit to LY-labeled myr-G $\alpha$  subunits. Fluorescence polarization at LY wavelengths was assessed with a Victor V multilabel plate reader (Perkin-Elmer Life Sciences, Boston, MA), and anisotropy was calculated as follows:

$$A = (S - GP)/(S + 2PG) \quad (1)$$

where  $A$  is anisotropy,  $S$  is polarized emission in the parallel direction,  $P$  is polarized emission in the perpendicular orientation, and  $G = 1.143$  for our system. The  $G$  factor, which corrects for disparities in the efficiency of light transmission in parallel and perpendicular positions, was determined experimentally.

Qualitative and quantitative binding of LY-labeled G $\alpha_i$  subunits to G $\beta\gamma$  was assessed with a FRET assay between G $\alpha_{i1}$ -LY and G $\beta\gamma$ -M8. M8 donor excitation (excitation at 320 nm and emission at 417 nm) resulted in an increase in LY emission (excitation at 430 nm and emission at 520 nm) upon subunit binding, less any contribution from G $\beta\gamma$ -M8 alone. The affinity of labeled G $\alpha$ -13CM-LY (4.1 nM) and G $\beta\gamma$ -M8 subunits was determined by addition of increasing amounts of G $\beta\gamma$ -M8 (0.6–30 nM). Binding resulted in a dose-dependent increase in LY emission. Qualitative binding was confirmed by measuring the fluorescence of G $\alpha$ -LY upon addition of a 1.5-fold molar excess of G $\beta\gamma$ -M8, and the percent increase in fluorescence was calculated as follows:

$$[(F_{G\alpha\beta\gamma} - F_{G\alpha})/F_{G\alpha}] \times 100 \quad (2)$$

where  $F_{G\alpha\beta\gamma}$  is the fluorescence emission of the reconstituted heterotrimer at 520 nm (excitation at 320 nm) and  $F_{G\alpha}$  is the emission measured in the absence of G $\beta\gamma$ -M8.

**Spin Labeling and EPR Measurements.** Spin labeling was carried out in a buffer containing 10 mM MES (pH 6.8), 100 mM NaCl, 5 mM MgCl<sub>2</sub>, 100  $\mu$ M GDP, and 10% glycerol (wt %). G $\alpha_i$  subunits (final concentration of 10  $\mu$ M) were incubated with the sulfhydryl spin-label S-(1-oxy-2,2,5,5-tetramethylpyrroline-3-methyl)methanethio-sulfonate in a 1:1 molar ratio at room temperature for ~2 h. Any unreacted label was removed by extensive washing using an Amicon concentrator with a molecular mass cutoff of 10 kDa. For EPR spectroscopy, the G $\alpha_i$  samples were loaded into an AquaX quartz 4 bore cell (Bruker Biospin, Billerica, MA). Spectra were recorded at X-band microwave frequencies using a Bruker E580 spectrometer and a high-sensitivity resonator (HS0118). Each spectrum was collected with a 100 G field scan, a modulation amplitude of 4 G at



100 kHz, and a microwave power of 19.92 mW. The recorded data are averages of 100 scans. After each  $G\alpha_i$  spectrum was collected, the sample was recovered and  $G\beta\gamma$  was added in equimolar amounts. The diluted solution was then concentrated to the original  $G\alpha_i$  concentration, and a spectrum was collected.

A spectrum of the 17R1 myristoylated mutant was also recorded at  $-50^\circ\text{C}$  using a quartz flat cell with a 110 G field scan and a microwave power of 0.1992 mW. The low-temperature spectrum was fit using a Levenberg–Marquardt rigid limit simulation program to obtain rigid limit magnetic parameters for EPR simulations. In addition, the hyperfine splitting parameters from the rigid limit spectrum were used to obtain the rotational correlation times of the nitroxide ( $\tau_c$ ) according to

$$\tau_c = a(1 - S)^b \quad (3)$$

where an  $a$  of  $8.52 \times 10^{-10}$  s and a  $b$  of  $-1.16$  are empirical values determined for a Brownian diffusion model with a 5 G Lorentzian line width (30, 31) and  $S$  is the ratio of the splitting of the outer hyperfine extrema in the slow motional ( $2A_{zz}'$ ) and rigid limit ( $2A_{zz}$ ).

The EPR spectra of the spin-labeled proteins were fit using the NLSL program of Freed and co-workers (32). For the 17R1 side chain, the principal values of the  $\mathbf{g}$  and  $\mathbf{A}$  tensors obtained by rigid limit simulation are as follows:  $g_{xx} = 2.0086$ ,  $g_{yy} = 2.0066$ ,  $g_{zz} = 2.0023$ ,  $A_{xx} = 6.2$ ,  $A_{yy} = 5.9$ , and  $A_{zz} = 37$ . These magnetic parameters were fixed in all simulations.

## RESULTS

**Strategy for Studying the Activation-Dependent Conformational Changes of the Myristoylated Amino Terminus of the  $G\alpha$  Subunit.** We previously addressed the role of the  $G\alpha$  amino terminus in G protein activation with a site-directed cysteine mutagenesis study of nonmyristoylated  $G\alpha$  subunits (25). The same amino-terminal Cys mutants were expressed as myristoylated proteins for use in the current studies in an effort to elucidate the role of myristoylation in the structure and function of  $G\alpha_i$  subunits. The cysteine mutations are located at multiple positions on the amino-terminal helix (Figure 1A), primarily at solvent-exposed positions opposite the  $G\beta\gamma$  binding interface. The proteins were coexpressed in *E. coli* with a plasmid encoding *N*-myristoyltransferase, purified by Ni–NTA chromatography (Figure 1B), followed by a final purification by ion exchange chromatography. *N*-Myristoyltransferase tolerates a variety of residues at position 3, and residues critical to the function of this enzyme, specifically the fifth and sixth residues, were preserved in all the Hexa I mutant proteins (33, 34).

All of the nine Hexa I Cys mutants were cotranslationally modified by NMT with  $\geq 85\%$  efficiency as evidenced by a faster migration of acylated proteins compared to the same nonmyristoylated mutant on SDS–PAGE gels in the presence of urea (11, 28). In the final purification by ion exchange chromatography, the myristoylated proteins eluted at a lower salt concentration than their nonmyristoylated counterparts (Figure 1C) which were excluded from the pool of active, myristoylated protein reserved for fluorescent and spin labeling (Figure 1D).

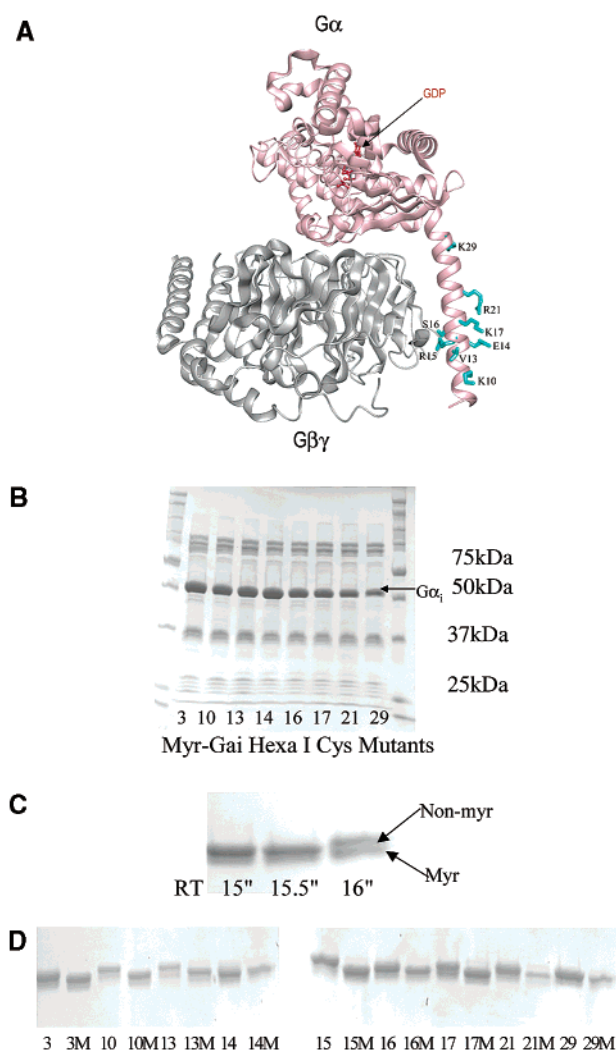


FIGURE 1: Expression and purification of myr- $G\alpha_i$  Hexa I proteins. (A) Visualization of  $G\alpha_i$  complexed with  $G\beta\gamma$  using DINO (PDB entry 1GP2) (25). (B) Coomassie-stained SDS–PAGE gel of Ni–NTA protein extracts (10 to 20% Tris–glycine gel). (C) Purification of the myristoylated protein prior to labeling. RT (retention time) is the length of time the sample was retained on the column. RT 15" describes the fraction which elutes 15 min after injection into the flow path. Aliquots of the fractions from chromatography were analyzed via SDS–PAGE. Lanes represent the profile from anion exchange fractions of the  $G\alpha_i$  Hexa I-17CM protein on a Coomassie-stained SDS–urea gel (10% Tris–glycine gel and 1 M urea). (D) SDS–urea gel of myristoylated (M) and nonmyristoylated  $G\alpha_i$  Hexa I proteins after HPLC purification.

**Functional Assays.** To determine whether the mutant proteins folded properly, had GDP bound, and could undergo a GTP-dependent conformational change, the intrinsic Trp fluorescence change after addition of  $\text{AlF}_4^-$  was measured. Similar to wild-type recombinant  $G\alpha_{i1}$ , all amino-terminal myristoylated  $G\alpha_i$  Hexa I proteins underwent a conformational change upon binding to  $\text{AlF}_4^-$ ; the  $G\alpha$  proteins exhibited an at least 40% increase in relative fluorescence both before and after labeling, demonstrating that the labeled proteins were properly folded and functional.

**Labeling of Myristoylated  $G\alpha_i$ -LY Hexa I Proteins.** Conformational changes associated with G protein activation were detected in fluorescent assays by attachment of a thiol reactive environmentally sensitive probe, LY (Figure 2A). After ion exchange chromatography, LY was used to specifically label each of the amino-terminal mutants.

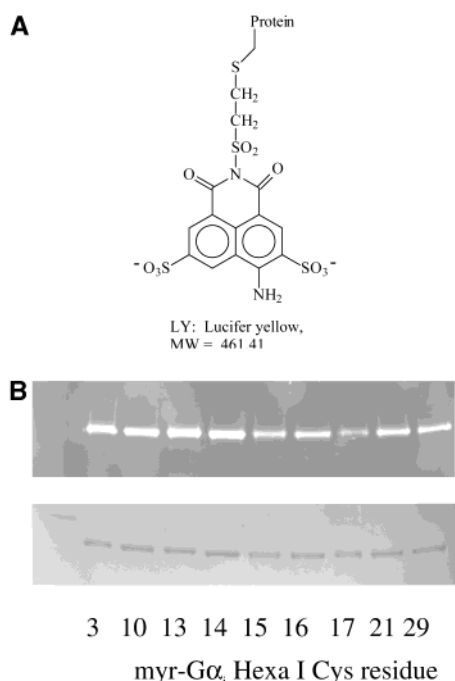


FIGURE 2: Fluorescent labeling of myr- $G\alpha_i$  Hexa I proteins. (A) Fluorescent probe, LY, used in this study. (B) UV illumination of LY-labeled myr- $G\alpha_i$  Hexa I proteins (top panel) and Coomassie stain (bottom panel) of purified, LY-labeled subunits on an SDS-PAGE 10 to 20% Tris-glycine gel.

Unreacted label was removed by gel filtration chromatography, and each protein was subjected to SDS-PAGE and detected by UV illumination and Coomassie staining (top and bottom panels of Figure 2B, respectively). Use of gel filtration chromatography with a calibrated column to isolate the labeled proteins ensured the monomeric state of the proteins, which is unchanged by  $AlF_4^-$  activation (25). To determine whether the mutant proteins folded properly, had GDP bound, and could undergo GTP-dependent conformational changes, the intrinsic Trp fluorescence change after addition of  $AlF_4^-$  was measured. The labeled proteins retained the ability to undergo activation; the increase in intrinsic Trp fluorescence of the LY-labeled proteins after the addition of  $AlF_4^-$  was again  $\sim 40\%$ , indicating proper functioning of these labeled subunits (29).

To further ensure proper functioning of labeled subunits, binding of LY-labeled myristoylated  $G\alpha_i$  to  $G\beta\gamma$  was confirmed by energy transfer between fluorescently labeled  $G\beta\gamma$  (donor) and  $G\alpha$ -LY (acceptor) subunits (35). Energy transfer resulted in a dose-dependent increase in acceptor emission upon binding of  $G\alpha_i$  Hexa I to 13CM-LY and of  $G\beta\gamma$  to M8, less any contributions from donor-labeled  $G\beta\gamma$ -M8 alone (Figure 3A). The measured  $K_d$  of 7 nM is consistent with the reported value for the interaction of myristoylated  $G\alpha$  with  $G\beta\gamma$  (36). Similar qualitative results were obtained for all labeled subunits (Figure 3B). The fluorescence of  $G\alpha_i$  Hexa I-15CM-LY increased markedly upon  $G\beta\gamma$  binding, consistent with its known position as a direct  $G\beta\gamma$  contact site on the heterotrimeric  $\alpha$ - $\beta\gamma$  interface (Figure 1A). Although both 15C and 16C are located at the  $G\alpha$ - $\beta\gamma$  binding interface, it is likely that 15C-LY is closer to a donor fluorophore on M8- $G\beta\gamma$  than 16C-LY, which shows a more modest increase in fluorescence upon  $G\beta\gamma$  binding.

**Effect of  $G\alpha$  Activation on the Fluorescence of Site Specific Fluorescent Labels.** To determine whether there was an activation-dependent conformational change in or around the myristoylated amino terminus of  $G\alpha$ , we first measured the fluorescence change of labeled amino-terminal myr- $G\alpha_i$ -LY mutants upon addition of  $AlF_4^-$  (Figure 4 and Table 1) at LY specific wavelengths. We found changes in the fluorescence of LY-labeled amino-terminal residues ranging from 0 to 40% for these residues upon activation. Figure 4A is a representative example of the data collected for  $G\alpha_i$  Hexa I-21CM-LY. Upon addition of  $AlF_4^-$  to the LY-labeled  $G\alpha_i$  Hexa I-21CM protein, the relative fluorescence increased  $\sim 30\%$ , indicating a more hydrophobic environment for this LY-labeled residue upon activation. Similar changes in fluorescence were seen for LY-labeled residues 15–17 located midway through the amino-terminal region (Figure 4B). There was a small but measurable change in LY fluorescence upon binding to  $G\beta\gamma$  for the myristoylated amino-terminal residues, indicating a move to a slightly more solvent-exposed environment upon activation, consistent with their solvent-exposed positions when bound to  $G\beta\gamma$  (Figure 4A and Table 1).  $AlF_4^-$  activation of the  $G\alpha_i$  Hexa I-21CM-LY- $G\beta\gamma$  complex increased LY fluorescence to the same extent as direct activation of the  $G\alpha$ GDP subunit, indicating quantitative dissociation of reconstituted heterotrimers (Figure 4A). All of the fluorescent changes exhibited by the labeled proteins were in contrast to control experiments with  $AlF_4^-$  added to (i) LY alone, (ii) a  $G\beta\gamma$ /LY mixture, (iii)  $G\beta\gamma$  alone, and (iv) a mixture of  $G\alpha$  and nonreactive LY, all of which showed no changes in fluorescence (25).

**Mobility of Myristoylated  $G\alpha_i$  Hexa I Proteins.** To determine the effect of myristoylation on amino-terminal mobility, the anisotropy of LY-labeled residues was examined in myristoylated and nonmyristoylated  $G\alpha_i$  Hexa I proteins. The anisotropy of LY-labeled  $G\alpha$  subunits was measured in 50% glycerol to isolate localized movement in and around the region of labeled residues without additional contributions from global tumbling of the molecule (37). The labeled proteins retained the ability to undergo activation in the presence of 50% glycerol; the increase in the intrinsic Trp fluorescence of the LY-labeled proteins after the addition of  $AlF_4^-$  was again  $\sim 40\%$ , indicating proper functioning of these labeled subunits (29) in the assay medium. The anisotropy values for myristoylated amino-terminal mutants were higher than those of the nonmyristoylated counterparts at all positions examined along the amino-terminal helix, both in the activated GDP- and  $AlF_4^-$ -bound state (Figure 5A) and in the inactive GDP- and  $G\beta\gamma$ -bound states (Figure 5B,C). This is consistent with an immobilized amino terminus in all conformations of  $G\alpha$ . While glycerol greatly reduces the extent of global tumbling of molecules, without time-resolved analysis we cannot rule out myristoylation as an additional contributor to the already reduced level of global tumbling. Nevertheless, this is likely to be small due to the fact that myristoylation has little effect on the size or weight of the  $G\alpha$  molecule itself. Figure 5D compares the anisotropy of myristoylated  $G\alpha_i$  Hexa I in different conformations. There is a small gradient of mobility along the  $\alpha$ -helix; however, it is relatively small compared to the larger effects of myristoylation itself on the anisotropy of  $G\alpha_i$  proteins (panels A–C vs panel D of Figure 5).

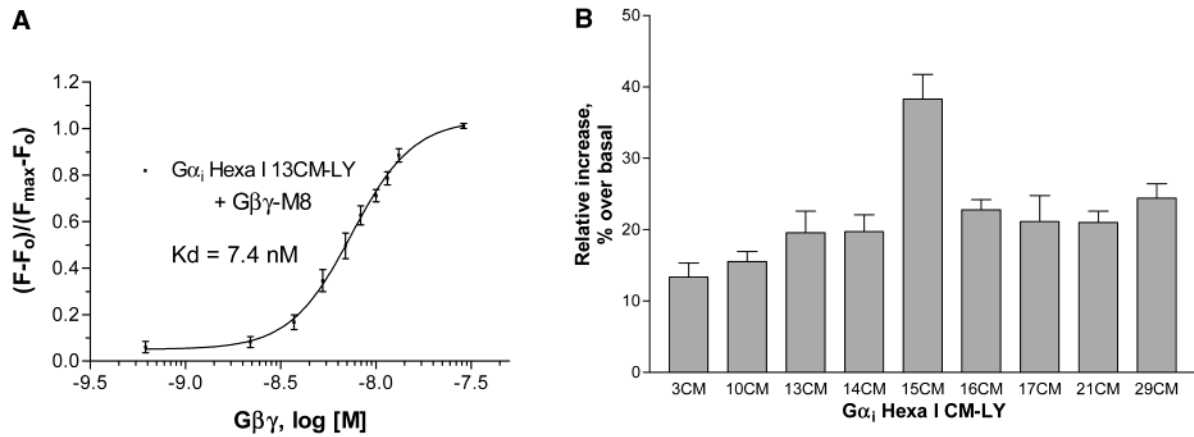


FIGURE 3: Binding of LY-labeled myr-Gα<sub>i</sub> Hexa I subunits (acceptor) to Gβγ-M8 (donor) results in energy transfer and increased acceptor emission (excitation at 320 nm and emission at 520 nm). All Gαβγ values less the contribution of an equimolar amount of Gβγ-M8 in the absence of GαCM-LY. (A) Increase in fluorescence relative to the maximum increase upon binding of Gβγ-M8 (0.6–30 nM) to Gα<sub>i</sub> Hexa I-13CM-LY (4.1 nM). Data are averages of four independent experiments. (B) Binding of excess Gβγ-M8 (8.8 nM) to Gα-LY (6.0 nM) subunits. Data are averages of three independent experiments.

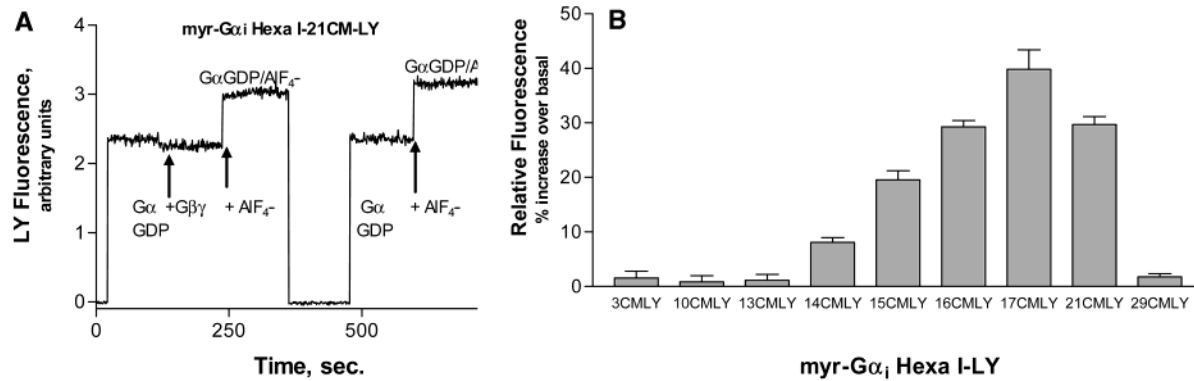


FIGURE 4: Gβγ-dependent and AlF<sub>4</sub><sup>-</sup>-dependent changes in specifically labeled Gα<sub>i</sub> Hexa I proteins (excitation at 430 nm and emission at 520 nm). (A) LY fluorescence of 50 nM Gα<sub>i</sub> Hexa I-V21CM-LY subunit upon binding to Gβγ (100 nM) and after AlF<sub>4</sub><sup>-</sup> activation of the reconstituted heterotrimer (left) or direct AlF<sub>4</sub><sup>-</sup> activation of GαGDP (right). (B) Activation-dependent relative increases in fluorescence for all labeled amino-terminal residues. Data are averages of three to five independent experiments.

Table 1: Summary of Fluorescent Changes for Myr-Gα<sub>i</sub> Hexa I-LY Proteins (% increase over basal)<sup>a</sup> (left) and Previous Results Utilizing Nonmyristoylated Proteins (right) (25)

myristoylated Gα <sub>i</sub> Hexa I-GDP	with AlF <sub>4</sub> <sup>-</sup>	with Gβγ	nonmyristoylated Gα <sub>i</sub> Hexa I-GDP	with AlF <sub>4</sub> <sup>-</sup>	with Gβγ
3CMLY	1.5 ± 1.6	-1.53	3CLY	3.0	19.0
10CMLY	0.9 ± 1.9	-3.87	10CLY	14.9	6.5
13CMLY	1.2 ± 2.1	-4.73	13CLY	13.5	18.2
14CMLY	8.1 ± 1.3	-1.74	14CLY	7.8	5.9
15CMLY	19.6 ± 2.3	-3.74	15CLY	3.2	-2.5
16CMLY	29.3 ± 2.0	-2.08	16CLY	4.9	10.9
17CMLY	39.8 ± 5.3	-3.25	17CLY	12.3	11.5
21CMLY	29.7 ± 2.1	-3.03	21CLY	20.8	13.2
29CMLY	1.8 ± 1.0	-2.95	29CLY	3.1	0.1

<sup>a</sup> LY fluorescence emission of labeled proteins was monitored at 520 nm with excitation at 430 nm. The percent increase in fluorescence is relative to the LY fluorescence of the GαGDP-bound subunit. Gβγ binding data are averages of two to three independent experiments.

**Electron Paramagnetic Resonance Spectroscopy of the Spin-Labeled Mutants.** To further examine the conformation of the Gα<sub>i</sub> amino terminus, myristoylated cysteine mutants in the Hexa I background were modified with a nitroxide methanethiosulfonate spin reagent to generate the spin-labeled side chain designated R1 (Figure 6A). Figure 6B shows the EPR spectra of nine Gα<sub>i</sub> R1 derivatives before and after the addition of Gβγ. All of the data have well-

resolved outer hyperfine extrema with a 2A<sub>zz</sub>' of ~68 G, indicative of a nitroxide in the slow motional regime. The rigid limit spectrum (data not shown) for the 17R1 mutant shows a 2A<sub>zz</sub> hyperfine splitting of 74 G. Rotational correlation times calculated using this value and eq 3 indicate that the rotational motion of the nitroxide (τ<sub>c</sub> = 16 ns) is similar to the tumbling rate of the protein computed from the Stokes–Einstein relationship (τ<sub>c</sub> ~ 14 ns).

Each of the EPR spectra apparently consists of two components arising from spin populations with different mobilities that vary in relative amounts from site to site. In this case, the individual components may be obtained by subtraction of one spectrum from another that differs in the relative amounts. For example, subtraction of the appropriate amount of the 14R1 spectrum from the 29R1 spectrum yields the mobile component spectrum (Figure 6C, bottom, green trace), and subtraction of this spectrum from that of 29R1 yields the spectrum of the immobile species (Figure 6C, middle panel, blue trace). These individual spectra were fit well with an isotropic diffusion model to give correlation times of approximately 1 and 16 ns for the mobile and immobile components, respectively (Figure 6C, bottom and middle panels, black traces). The spectrum of 29R1 is best fit by a state with 39% of the spin arising from the mobile population (Figure 6C, top panel, black trace). Similar



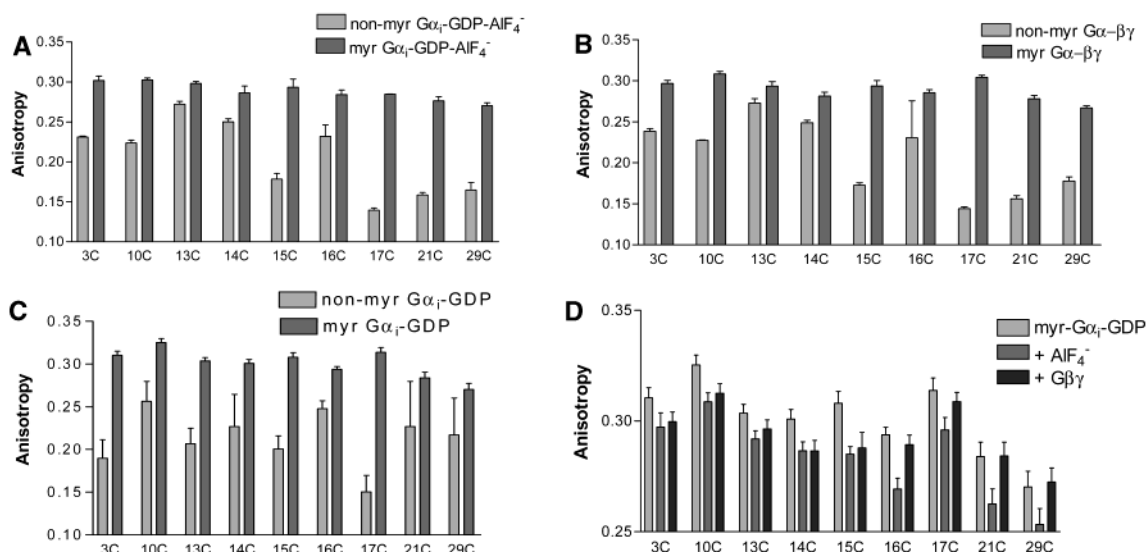


FIGURE 5: Effect of myristoylation on the mobility of  $G\alpha_i$  Hexa I-LY proteins labeled at the indicated amino-terminal residues. Fluorescence anisotropy of myristoylated and nonmyristoylated LY-labeled  $G\alpha_i$  subunits (200 nM) in buffer B calculated from fluorescence polarization obtained with the Victor multilabel plate reader upon addition of (A)  $AIF_4^-$  (10 mM NaF and 50  $\mu$ M  $AlCl_3$ ) or (B)  $G\beta\gamma$  (400 nM). (C) Anisotropy of GDP-bound myristoylated and nonmyristoylated  $G\alpha_i$  subunits. (D) Anisotropy of myristoylated proteins in the myr- $G\alpha_i$ -GDP-, myr- $G\alpha_i\beta\gamma$ -, and myr- $G\alpha_i$ -GDP- $AIF_4^-$ -bound state. All data are averages of three or more independent experiments.

analyses of the other mutants showed that the more mobile component constituted 20–40% of the population, and had a correlation time in the range of 1–4 ns. The immobile population was consistently 16 ns. The values for the mobile component are approximate due to the high modulation amplitude used to enhance detection sensitivity for the dominant immobilized component. It is evident from the data of Figure 6B that there is little change in the spectra of myristoylated  $G\alpha_i$  (black traces) upon interaction with  $G\beta\gamma$  (red traces). The spectral changes that are seen reflect small changes in the ratio of the mobile and immobile populations.

To rule out aggregation as an artifactual cause of reduced mobility in the predominantly immobile population of myr- $G\alpha_i$  subunits, gel filtration chromatography was performed on representative samples of myristoylated proteins. Retention times for these subunits before and after spin labeling were consistent with monomeric  $G\alpha_i$ , with a molecular mass of  $\sim$ 40 kDa, compared to a mass of 66 kDa for the monomeric albumin standard.

## DISCUSSION

The amino terminus of  $G\alpha$  subunits plays complex roles in activation and deactivation of G proteins. Myristate, an integral component of all  $G\alpha_i$  family members, adds another level of complexity to G protein signaling. The slow step in G protein activation involves release of GDP. The activation process could involve the amino terminus by either direct contacts or a relative movement of the helical and GTPase domains of  $G\alpha$ . A shift between domains may widen a cleft that eases nucleotide release, and this may involve specific interactions between the amino and carboxy termini (38–40). A  $G\alpha_i$ -like chimera that perturbs the interaction between amino-terminal Val<sup>30</sup> and carboxy-terminal Ile<sup>339</sup> increases the extent of GDP release, while adding a contact in the hydrophobic pocket to break the interaction between the  $\alpha$ -helical and GTPase domain (His<sup>41</sup>Val) reduces the extent of basal GDP release (38). These results suggest the relative

orientation between amino and carboxy domains regulates the basal activity of these subunits.

To determine the function of myristate in G protein activation and deactivation, EPR and fluorescence studies have compared nonmyristoylated (25) and myristoylated proteins. While both studies reveal changes in amino-terminal structure upon formation of the inactive heterotrimer, as well as during activation of  $G\alpha_i$  subunits, the study presented here demonstrates a number of prominent differences between myristoylated and nonmyristoylated  $G\alpha_i$  proteins, suggesting a critical role for myristoylation in the structure and function of  $G\alpha$  subunits.

EPR spectra of nonmyristoylated  $G\alpha_i$ -GDP reveal a dynamic random coil-like state for the amino terminus. Only upon complexation with  $G\beta\gamma$  to form the inactive heterotrimer are the spectra consistent with an  $\alpha$ -helical structure (25). This is not the case for myristoylated  $G\alpha_i$  proteins. EPR spectra of the spin-labeled, myristoylated  $G\alpha_i$ -GDP reveal that the dominant population of the spin-label R1 side chain is uniformly immobilized along the length of the amino terminus, in contrast to the highly mobile side chain in the nonmyristoylated counterparts (25). Because the spin-labeled  $G\alpha_i$  subunits do not appear to be aggregated, it must be concluded that the amino terminus adopts a highly ordered structure. The strong immobilization of all side chains that have been examined indicates tertiary interactions of the amino-terminal sequence along its length, and precludes a dynamic analysis of the nitroxide motion that would allow a determination of the secondary structure.

As illustrated in Figure 6B, each spectrum of the myristoylated amino-terminal labeled protein is characterized by two components corresponding to a highly mobile and immobilized state. The immobilized state is always dominant, and has a correlation time of  $\sim$ 16 ns, corresponding to the rotational correlation time of  $G\alpha_i$  estimated from Stokes–Einstein behavior. Thus, it is highly immobilized with respect to the protein, and in strong tertiary interaction. On the other hand, the short correlation time of the more mobile compo-



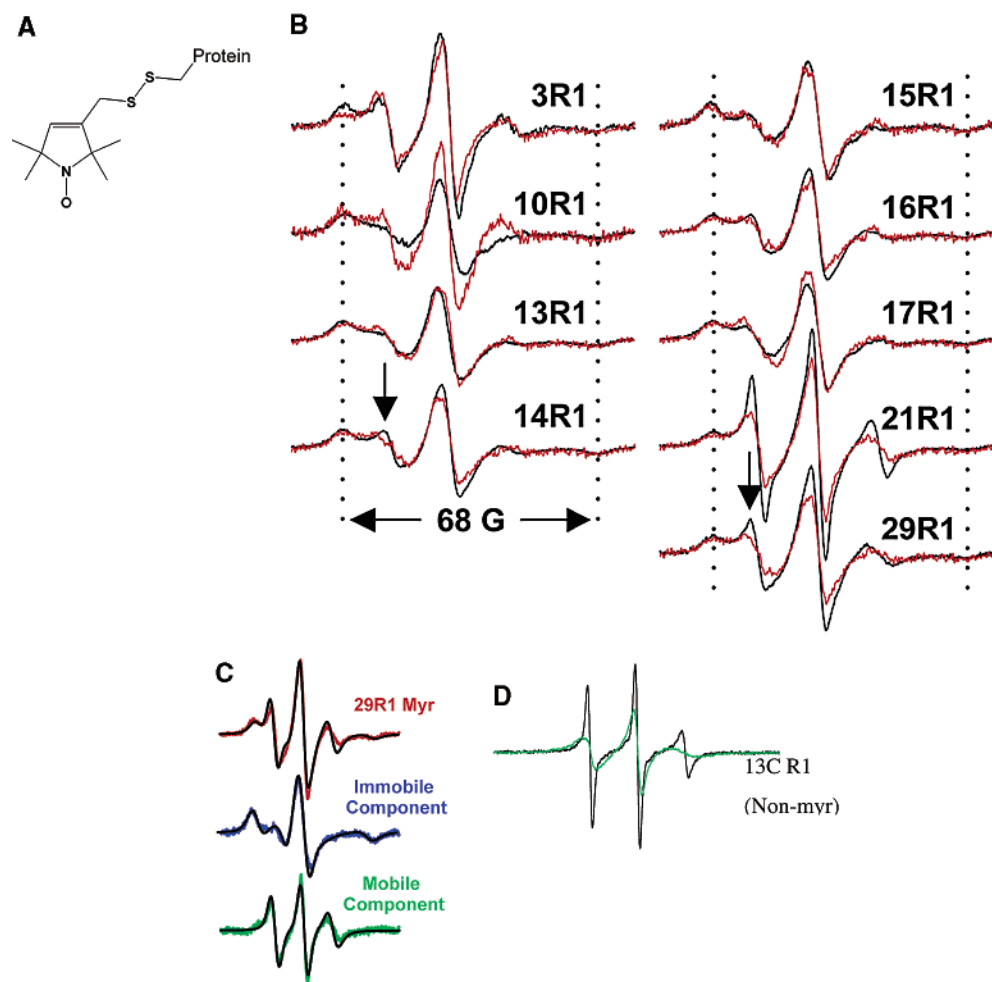


**FIGURE 6:** Electron paramagnetic resonance of the R1 side chain in  $G\alpha_i$ . (A) Structure of the side chain. (B) Normalized EPR spectra of nine  $G\alpha_i$  Hexa I CM-R1 labeled proteins along the myristoylated amino terminus of  $G\alpha_i$ , in the absence (black traces) and presence (red traces) of  $G\beta\gamma$ . The vertical dotted lines show the splittings of the outer hyperfine extrema, separated by 68 G. The arrows denote the locations of a relatively mobile component in the spectra. (C) Normalized EPR spectra of 29R1 (top panel, red trace) and the resolved mobile (green trace, bottom panel) and immobile (blue trace, middle panel) components. Simulated spectra are shown as superimposed black traces (see the text). (D) For comparison, spectra of nonmyristoylated  $G\alpha_i$  Hexa I-13C-R1 in the absence (black trace) and presence (green trace) of  $G\beta\gamma$  (25).

nent (1–4 ns) suggests that this state may represent a less ordered form of the amino terminus in equilibrium with the ordered state, or possibly two rotamers of the nitroxide side chain with different mobilities. The mobile component apparently does not arise from the nonmyristoylated protein, both because the population of this component (20–40%) exceeds the estimated level of the nonmyristoylated contaminant (<15%) and because its spectrum does not match that of unmyristoylated  $G\alpha_i$ GDP (Figure 6D) (25).

In the G protein cycle,  $G\alpha$ GTP is hydrolyzed to  $G\alpha$ GDP, and association with  $G\beta\gamma$  returns the  $G\alpha$  protein to its inactive, heterotrimeric state. The EPR spectra of myristoylated  $G\alpha$ GDP, upon addition of  $G\beta\gamma$ , reflect very little change, compared to spectra of nonmyristoylated  $G\alpha$  proteins (Figure 6B,D). This indicates that the dynamics and environment of the spin-labels do not change detectably upon formation of the complex. In turn, this implies that a structural rearrangement involving changes in tertiary interaction along the amino terminus is not detected upon complexation. Because the estimated correlation time of the spin-label in  $G\alpha_i$  apparently reflects the rotational diffusion of the subunit, it might be expected that complex formation should minimally reveal a spectral change due to a reduction

in the rotational diffusion rate. However, the nitroxide motion is already in the slow motional regime, and the great breadth of the outer hyperfine extrema, probably because of heterogeneity of the local environment, precludes detection of the slight reduction in line width expected from the approximate doubling of the molecular mass. It also follows that changes in protein internal dynamics with effective correlation times longer than  $\sim 20$  ns will not be readily detected in the linear EPR line shapes. Thus, modulation of low-frequency dynamic modes upon complexation of  $G\alpha_i$  with  $G\beta\gamma$  would escape detection.

Consistent with the EPR results, steady state fluorescence also revealed only small changes upon  $G\beta\gamma$  binding, despite a nanomolar binding affinity of LY-labeled  $G\alpha$  subunits for  $G\beta\gamma$  (Figure 3A). The small fluorescence decreases seen upon heterotrimer formation in myristoylated  $G\alpha$  proteins indicate a slightly more solvent-exposed environment for these labeled residues upon  $G\beta\gamma$  association, as would be expected for solvent-exposed amino-terminal residues moving out toward the bulk of the solution opposite the  $G\beta\gamma$  binding interface. This is in contrast to the nonmyristoylated proteins which demonstrate pronounced increases in fluorescence upon  $G\beta\gamma$  binding, suggesting a hydrophilic

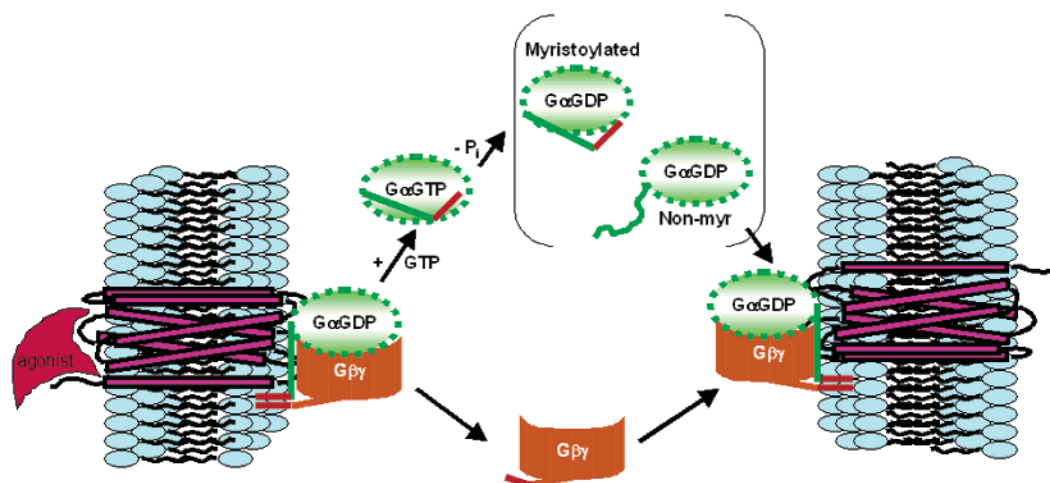


FIGURE 7: Hypothetical model of  $G\alpha$  amino-terminal involvement in G protein cycling. The agonist-occupied receptor activates G proteins, causing release of GDP, uptake of GTP, and dissociation of subunits. In the deactivation of G proteins,  $G\alpha$  hydrolyzes GTP to GDP, followed by reassociation of subunits and membrane binding. This work suggests the myristoylated amino terminus has an intramolecular binding site that rigidifies its structure. To reassociate with  $G\beta\gamma$ , there must be a transition of this region to an extended helix for  $\beta\gamma$  binding. The disordered amino terminus seen in nonmyristoylated  $G\alpha_i$  may be indicative of a transient intermediate before or during reassociation with  $G\beta\gamma$ . The farnesyl group of  $G\gamma$  and myristoyl group of  $G\alpha$  are both shown in red.  $G\alpha$  amino-terminal residues 1–30 are shown as a solid green line.

environment for these residues in the  $G\alpha$ GDP compared to the  $\beta\gamma$ -bound state (Table 1).

Since the EPR spectra demonstrated a highly immobilized state for the myristoylated amino terminus as compared to the nonmyristoylated amino terminus, we further explored the mobility of this region with fluorescence anisotropy of the LY-labeled  $G\alpha$  proteins. Fluorescence anisotropy is indicative of the average environment and mobility of labeled residues in solution. The highly immobilized state was also reflected in the steady state anisotropy studies, suggesting a restricted mobility of labeled residues for both the myr- $G\alpha$ GDP- and myr- $G\alpha$ GDP- $\text{AIF}_4^-$ -bound states at all positions examined along the amino terminus. These results also paint a picture of amino-terminal residues in a highly restricted rotational environment in myristoylated proteins, compared to nonmyristoylated proteins. Results of fluorescence and EPR demonstrate a significant stabilizing role for myristoylation in amino-terminal structure.

In this solution structure, the amino-terminal region may reside close to the rest of the molecule in the  $G\alpha$ GDP-bound state. However movement of these residues, either alone or in combination with conformational changes in the rest of the molecule, may change the local environment of amino-terminal residues, giving rise to the substantial activation-dependent increases in fluorescence seen for residues 14–17 and 21. These changes indicate a more hydrophobic environment for these residues upon activation, especially for residues midway through this 30-amino acid region. This is consistent with the activation-dependent fluorescence changes seen previously with nonmyristoylated proteins, where extended probes may stand in for myristate and stabilize this interaction (25).

Conformational changes in the amino terminus of  $G\alpha$  proteins could regulate movement of  $G\alpha$  proteins within the cell. Seitz et al. (41) found that the extent of binding of  $G\alpha_i$ -GTP to lipid monolayers is substantially lower than that of the  $G\alpha_i$ GDP subunit, indicating a difference in the hydrophobicity of the protein between the active and inactive state. Similarly, native  $G\alpha_i$ GDP in retinal membrane preparations

can be extracted into isotonic buffer containing GTP (20), indicating an increase in solubility for this myristoylated subunit in the active conformation. Receptor-mediated activation of  $G\alpha_i$  results in its redistribution from membrane to cytosol, accompanied by an increased level of depalmitoylation of  $G\alpha_i$  (42). The high degree of immobility seen in EPR spectra, the immobility suggested by anisotropy, and the activation-dependent increases in the hydrophobic environment seen in steady state fluorescence studies altogether suggest the possibility of an intramolecular binding site on the surface of the  $G\alpha$  molecule for the myristoylated amino terminus.

The idea of an intramolecular binding site for the amino terminus is not an entirely new one. The monoclonal antibody LAS-2 amino-terminal epitope includes residues 10–17, and the myristoyl group is close to these residues (43). LAS-2 binds myristoylated  $G\alpha_i$  proteins preferentially (43), as does Mab4A (44), indicating a difference in conformation between myristoylated and nonmyristoylated proteins. Our results support this hypothesis and include myristoylation as an essential feature of the structural changes in this region. Furthermore, an activation-dependent amino-terminal conformational change may be accompanied by an intramolecular binding site for the myristoylated amino terminus of  $G\alpha$ . Studies designed to locate an intramolecular binding site are underway, using protein docking simulations to guide creation of double-cysteine mutations in  $G\alpha$ . These double-cysteine mutants can be modified with a single type of probe prior to use in FRET-based anisotropy homotransfer assays and spin–spin EPR studies to identify the intramolecular binding site.

A hypothetical model of amino-terminal involvement in G protein activation is shown in Figure 7. The inactive heterotrimer, with its isoprenylated  $G\gamma$  and myristoylated  $G\alpha$ , binds membranes cooperatively (20). Agonist activation of the receptor triggers GDP release from the G protein, binding of GTP, and dissociation of subunits. A conformational change occurs upon  $G\alpha$  activation in switch and amino-terminal regions (25, 29), as well as carboxy-terminal

regions (1). This conformational change in the amino terminus may help facilitate dissociation of  $G\alpha_i$ GTP from  $G\beta\gamma$  and the receptor. This conformational change may also protect the myristoyl group from the cytosol, increasing the solubility of  $G\alpha$  and allowing it to translocate from the membrane to interact with effectors, regulators, or signaling rafts. The myristoylated amino terminus of  $G\alpha$  is shown participating in an intramolecular interaction with the surface of the  $G\alpha$  molecule in the  $G\alpha$ GTP-bound state, and to a lesser extent in the physiologically transient  $G\alpha$ GDP species (Figure 7). The nonmyristoylated  $G\alpha_i$ GDP random coil amino-terminal structure may represent a transient intermediate for the amino-terminal conformation between GTP-bound and inactive,  $G\beta\gamma$ -bound states.

Palmitoylation, a reversible lipidation, has the potential to dramatically affect the membrane association–dissociation cycle of  $G\alpha$  subunits. The intermediate hydrophobicity of myristate is only marginally able to effect membrane localization in the absence of cooperative association with  $G\gamma$ 's isoprenylated C-terminus (20). Bourne and co-workers have shown that myristoylated, palmitoylated  $G\alpha$  resides on the membrane (45); thus, regulation of palmitoylation will play a key role in interaction of  $G\alpha$  with  $\beta\gamma$  and membranes, and will help regulate interaction with other signaling partners (16).

The activation-induced fluorescence changes suggest the amino terminus serves as an activation-dependent myristoyl switch in  $G\alpha_i$  proteins. This was also suggested by previous results utilizing large, extended probes attached to amino-terminal residues in nonmyristoylated proteins which showed smaller but consistent changes upon activation (25). Several well-studied examples of myristoyl switch proteins are found in nature, including recoverin, ARF1, MARCKS, and PKA. The retinal protein recoverin acts as a calcium–myristoyl switch; once calcium binds, the myristoylated amino terminus flips out, allowing translocation of this protein to the membrane (46–49). The structure of PKA shows the myristoylated amino terminus buried in a hydrophobic pocket on the PKA enzyme (50). Phosphorylation and myristoylation of PKA act in opposite manners to potentiate this myristoyl–electrostatic switch (51). MARCKS may also function as a myristoyl–electrostatic switch; phosphorylation of the amino terminus causes its release from membranes (52).

ADP ribosylation factors are the only members of the small GTPase superfamily that contain a myristoylated amino-terminal extension. ARF1 may best depict an activation-dependent myristoyl switch. ARF1 is known to bind to membranes in a GTP-dependent manner, and uses its myristoylated amino terminus as a GTP-sensitive myristoyl switch (48, 49). Interestingly, this small G protein has also been shown to bind  $G\beta\gamma$  with a micromolar affinity in the presence of lipids (53). Thus, both ARF1 and heterotrimeric G proteins bind and hydrolyze GTP, are myristoylated at their amino termini, and bind  $G\beta\gamma$ . What could be the functional role of such a GTP–myristoyl switch in the G protein cycle? We speculate that this could be a part of a concerted mechanism for GTP-dependent dissociation of  $G\alpha$  from  $\beta\gamma$  subunits and from activated receptors. In addition, it could play roles in association with effectors, RGS proteins, or signaling rafts in the spatial and temporal regulation of G protein signaling.

The EPR and fluorescence together suggest myristoylation radically alters the structure and stability of the amino-terminal region, in comparison to previously studied nonmyristoylated proteins. These results are consistent with an immobile amino terminus in the GDP-bound state which moves into a more nonpolar environment upon activation. Fluorescence results revealed pronounced changes in the overall average polarity seen by fluorescent probes attached to the Cys residues upon activation. These solution studies also reveal the potential for an intramolecular binding site for the myristoylated amino terminus of  $G\alpha_i$  proteins. Further work in examining amino-terminal conformational changes in the presence of the membrane-bound receptor is underway. These crucial experiments will help illuminate any contributions from the amino terminus in receptor-mediated activation of G proteins, and allow us to examine conformational changes in a lipid environment. Until crystallographic studies reveal the exact position of the myristoylated amino terminus in GDP- and GTP-bound states, solution studies can be used to help determine the relative environment of residues in the myristoylated amino terminus as it dynamically cycles through activation and deactivation.

## ACKNOWLEDGMENT

We thank Dr. Christian Altenbach for providing the EPR rigid limit simulation program. We also thank Dr. Maurine Linder for the  $G\alpha_i$  and pbb131 vectors and Dr. Jurgen Vanhauwe for expert technical assistance.

## REFERENCES

1. Yang, C. S., Skiba, N. P., Mazzoni, M. R., and Hamm, H. E. (1999) Conformational changes at the carboxyl terminus of  $G\alpha$  occur during G protein activation, *J. Biol. Chem.* 274, 2379–2385.
2. Lambright, D. G., Noel, J. P., Hamm, H. E., and Sigler, P. B. (1994) Structural determinants for activation of the  $\alpha$ -subunit of a heterotrimeric G protein, *Nature* 369, 621–628.
3. Noel, J. P., Hamm, H. E., and Sigler, P. B. (1993) The 2.2 Å crystal structure of transducin- $\alpha$  complexed with GTP $\gamma$ S, *Nature* 366, 654–663.
4. Coleman, D. E., Berghuis, A. M., Lee, E., Linder, M. E., Gilman, A. G., and Sprang, S. R. (1994) Structures of active conformations of  $G\alpha_{i1}$  and the mechanism of GTP hydrolysis, *Science* 265, 1405–1412.
5. Mixon, M. B., Lee, E., Coleman, D. E., Berghuis, A. M., Gilman, A. G., and Sprang, S. R. (1995) Tertiary and quaternary structural changes in  $G\alpha_{i1}$  induced by GTP hydrolysis, *Science* 270, 954–960.
6. Wang, J., Frost, J. A., Cobb, M. H., and Ross, E. H. (1999) Reciprocal signaling between heterotrimeric G proteins and the p21-stimulated protein kinase, *J. Biol. Chem.* 274, 31641–31647.
7. Graf, R., Mattera, R., Codina, J., Estes, M. K., and Birnbaumer, L. (1992) A truncated recombinant  $\alpha$  subunit of  $G_{i3}$  with a reduced affinity for  $\beta\gamma$  dimers and altered guanosine 5'-3-O-(thio)-triphosphate binding, *J. Biol. Chem.* 267, 24307–24314.
8. Lambright, D. G., Sondek, J., Bohm, A., Skiba, N. P., Hamm, H. E., and Sigler, P. B. (1996) The 2.0 Å crystal structure of a heterotrimeric G protein, *Nature* 379, 311–319.
9. Wall, M. A., Coleman, D. E., Lee, E., Iniguez-Lluhi, J. A., Posner, B. A., Gilman, A. G., and Sprang, S. R. (1995) The structure of the G protein heterotrimer  $G\alpha_{i1}\beta_1\gamma_2$ , *Cell* 83, 1047–1058.
10. Resh, M. D. (1999) Fatty acylation of proteins: new insights into membrane targeting of myristoylated and palmitoylated proteins, *Biochim. Biophys. Acta* 1451, 1–16.
11. Linder, M. E., Pang, I. H., Duronio, R. J., Gordon, J. I., Sternweis, P. C., and Gilman, A. G. (1991) Lipid modifications of G protein subunits. Myristoylation of  $G\alpha$  increases its affinity for  $\beta\gamma$ , *J. Biol. Chem.* 266, 4654–4659.



12. Kokame, K., Fukada, Y., Yoshizawa, T., Takao, T., and Shimonishi, Y. (1992) Lipid modification at the N terminus of photoreceptor G-protein  $\alpha$ -subunit, *Nature* 359, 749–752.
13. Casey, P. J., Graziano, M. P., and Gilman, A. G. (1989) G protein  $\beta\gamma$  subunits from bovine brain and retina: equivalent catalytic support of ADP-ribosylation of  $\alpha$  subunits by pertussis toxin but differential interactions with G $\alpha_s$ , *Biochemistry* 28, 611–616.
14. van der Neut, R., Pantaloli, C., Nebout, I., Bockaert, J., and Audigier, Y. (1993) Mutagenesis of the amino terminal glycine to alanine in G $\alpha_s$  subunit alters  $\beta\gamma$  dependent properties and decreases adenyllyl cyclase activation, *J. Biol. Chem.* 268, 436–441.
15. Galbiati, F., Guzzi, F., Magee, A. I., Milligan, G., and Parenti, M. (1996) Chemical inhibition of myristoylation of the G-protein G $\alpha_{i1}$  by 2-hydroxymyristate does not interfere with its palmitoylation or membrane association. Evidence that palmitoylation, but not myristoylation, regulates membrane attachment, *Biochem. J.* 313, 717–720.
16. Moffett, S., Brown, D. A., and Linder, M. E. (2000) Lipid-dependent targeting of G proteins into rafts, *J. Biol. Chem.* 275, 2191–2198.
17. Song, K. X., Sargiacomo, M., Galbiati, F., Parenti, M., and Lisanti, M. P. (1997) Targeting of a G $\alpha$  subunit (G $\alpha_{i1}$ ) and c-Src tyrosine kinase to caveolae membranes: clarifying the role of N-myristoylation, *Cell. Mol. Biol.* 43, 293–303.
18. Wise, A., and Milligan, G. (1997) Rescue of functional interactions between the  $\alpha$ 2a-adrenoreceptor and acylation-resistant forms of G $\alpha_{i1}$  by expressing the proteins from chimeric open reading frames, *J. Biol. Chem.* 272, 24673–24678.
19. Wilson, P. T., and Bourne, H. R. (1995) Fatty acylation of  $\alpha_z$  effects of palmitoylation and myristoylation on  $\alpha_z$  signaling, *J. Biol. Chem.* 270, 9667–9675.
20. Bigay, J., Faurobert, E., Franco, M., and Chabre, M. (1994) Roles of lipid modifications of transducin subunits in their GDP-dependent association and membrane binding, *Biochemistry* 33, 14081–14090.
21. Wang, Y., Windh, R. T., Chen, C. A., and Manning, D. R. (1999) N-Myristoylation and  $\beta\gamma$  play roles beyond anchorage in the palmitoylation of the G protein  $\alpha(o)$  subunit, *J. Biol. Chem.* 274, 37435–37442.
22. Gallego, C., Gupta, S. K., Winitz, S., Eisfelder, B. J., and Johnson, G. L. (1992) Myristoylation of the G $\alpha_{i2}$  polypeptide, a G protein  $\alpha$  subunit, is required for its signaling and transformation functions, *Proc. Natl. Acad. Sci. U.S.A.* 89, 9695–9699.
23. Mazzoni, M. R., Malinski, J. A., and Hamm, H. E. (1991) Structural analysis of rod GTP-binding protein, G $_t$ . Limited proteolytic digestion pattern of G $_t$  with four proteases defines monoclonal antibody epitope, *J. Biol. Chem.* 266, 14072–14081.
24. Skiba, N. P., Bae, H., and Hamm, H. E. (1996) Mapping of effector binding sites of transducin  $\alpha$ -subunit using G $\alpha_{i1}$  chimeras, *J. Biol. Chem.* 271, 413–424.
25. Medkova, M., Preininger, A. M., Yu, N. J., Hubbell, W. L., and Hamm, H. E. (2002) Conformational changes in the amino-terminal helix of the G protein  $\alpha_{i1}$  following dissociation from G $\beta\gamma$  subunit and activation, *Biochemistry* 41, 9962–9972.
26. Bradford, M. M. (1976) A rapid and sensitive method for the quantitation of microgram quantities of protein utilizing the principle of protein-dye binding, *Anal. Biochem.* 72, 248–254.
27. Phillips, W. J., and Cerione, R. A. (1991) Labeling of the  $\beta\gamma$  subunit complex of transducin with an environmentally sensitive cysteine reagent. Use of fluorescence spectroscopy to monitor transducin subunit interactions, *J. Biol. Chem.* 266, 11017–11024.
28. Mumby, S. M., and Linder, M. E. (1994) Myristoylation of G-protein  $\alpha$  subunits, *Methods Enzymol.* 237, 255–268.
29. Mazzoni, M. R., and Hamm, H. E. (1993) Tryptophan207 is involved in the GTP-dependent conformational switch in the  $\alpha$  subunit of the G protein transducin: chymotryptic digestion patterns of the GTP $\gamma$ S and GDP-bound forms, *J. Protein Chem.* 12, 215–221.
30. Goldman, S. A., Bruno, G. V., and Freed, J. H. (1972) *J. Phys. Chem.* 76, 1858–1860.
31. Freed, J. H. (1976) in *Spin Labeling: Theory and Application* (Berliner, L. J., Ed.) pp 53–132, Academic Press, New York.
32. Budil, D. E., Lee, S., Saxena, S., and Freed, J. H. (1996) Nonlinear-least-squares analysis of slow motion EPR spectra in one and two dimensions using a modified Levenberg-Marquart algorithm, *J. Magn. Reson., Ser. A* 120, 155–189.
33. Towler, D. A., Adams, S. P., Eubanks, S. R., Towery, D. S., Jackson-Machelski, E., Glaser, L., and Gordon, J. I. (1987) Purification and characterization of yeast myristoyl CoA:protein N-myristoyl transferase, *Proc. Natl. Acad. Sci. U.S.A.* 84, 2708–2712.
34. Duronio, R. J., Jackson-Machelski, E., Heuckeroth, R. O., Olins, P. O., Devine, C. S., Yonemoto, W., Slice, L. W., Taylor, S. S., and Gordon, J. I. (1990) Protein N-myristoylation in *Escherichia coli*: reconstitution of a eukaryotic protein modification in bacteria, *Proc. Natl. Acad. Sci. U.S.A.* 87, 1506–1510.
35. Mittal, R., Cerione, R. A., and Erickson, J. W. (1994) Aluminum fluoride activation of bovine transducin induces two distinct conformational changes in the  $\alpha$  subunit, *Biochemistry* 33, 10178–10184.
36. Sarvazyan, N. A., Remmers, A. E., and Neubig, R. R. (1998) Determinants of G $\alpha_{i1}$  and  $\beta\gamma$  binding. Measuring high affinity interactions in a lipid environment using flow cytometry, *J. Biol. Chem.* 273, 7934–7940.
37. Lakowicz, J. R. (1999) *Principles of fluorescence spectroscopy*, 2nd ed., Kluwer Academic/Plenum Publishers, Dordrecht, The Netherlands.
38. Muradov, K. G., and Artemyev, N. O. (2000) Coupling between the N- and C-terminal domains influences transducin- $\alpha$  intrinsic GDP/GTP exchange, *Biochemistry* 39, 3937–3942.
39. Remmers, A. E., Engel, C., Liu, M., and Neubig, R. R. (1999) Interdomain interactions regulate GDP release from heterotrimeric G proteins, *Biochemistry* 38, 13795–13800.
40. Thomas, T. O., Bae, H., Medkova, M., and Hamm, H. E. (2001) An intramolecular contact in G $\alpha$  transducin that participates in maintaining intrinsic GDP release rate, *Mol. Cell Biol. Res. Commun.* 4, 282–291.
41. Seitz, H. R., Heck, M., Hofmann, K. P., Alt, T., Pellaud, J., and Seelig, A. (1999) Molecular determinants of the reversible membrane anchorage of the G-protein transducin, *Biochemistry* 38, 7950–7960.
42. Wedegaertner, P. B., and Bourne, H. R. (1994) Activation and depalmitoylation of G $\alpha_s$ , *Cell* 77, 1063–1070.
43. Justice, J. M., Bliziotis, M. M., Stevens, L. A., Moss, J., and Vaughan, M. (1995) Involvement of N-myristoylation in monoclonal antibody recognition on chimeric G protein  $\alpha$  subunits, *J. Biol. Chem.* 270, 6436–6439.
44. Mazzoni, M. R., and Hamm, H. E. (1989) Effect of monoclonal antibody binding on  $\alpha$ - $\beta\gamma$  subunit interactions in the rod outer segment G protein, G $_b$ , *Biochemistry* 28, 9873–9880.
45. Morales, J., Fishburn, C. S., Wilson, P. T., and Bourne, H. R. (1998) Plasma membrane localization of G  $\alpha_z$  requires two signals, *Mol. Biol. Cell* 10, 1–14.
46. Ames, J. B., Tanaka, T., Ikura, M., and Streyer, L. (1995) Nuclear magnetic resonance evidence for a calcium induced extrusion of the myristoyl group of recoverin, *J. Biol. Chem.* 270, 30909–30913.
47. Tanaka, T., Ames, J. B., Harvey, T. S., Stryer, L., and Ikura, M. (1995) Sequestration of the membrane targeting myristoyl group of recoverin in the calcium-free state, *Nature* 376, 444–447.
48. Serafini, T., Orci, L., Amherdt, M., Brunner, M., Kahn, R. A., and Rothman, J. E. (1991) ADP ribosylation factor is a subunit of the golgi derived COP-coated vesicles: a novel role for a GTP binding protein, *Cell* 67, 239–253.
49. Franco, M., Chardin, P., Chabre, M., and Paris, S. (1995) Myristoylation of ADP-ribosylation factor 1 facilitates nucleotide exchange at physiological Mg $^{2+}$  levels, *J. Biol. Chem.* 270, 1337–1341.
50. Zheng, J., Knighton, D. R., Xuong, N. H., Taylor, S. S., Sowadski, J. M., and Ten Eyck, L. F. (1993) Crystal structures of the myristylated catalytic subunit of cAMP-dependent protein kinase reveal open and closed conformations, *Protein Sci.* 2, 1559–1573.
51. Tholey, A., Pipkorn, R., Bossemeyer, D., Kinzel, V., and Reed, J. (2001) Influence of myristoylation, phosphorylation, and deamidation on the structural behavior of the N-terminus of the catalytic subunit of CAMP-dependent protein kinase, *Biochemistry* 40, 225–231.
52. McLaughlin, S., and Adare, A. (1995) The myristoyl-electrostatic switch: a modulator of reversible protein-membrane interactions, *Trends Biochem. Sci.* 20, 272–276.
53. Franco, M., Paris, S., and Chabre, M. (1995) The small G-protein ARF1-GDP binds to the G $\beta\gamma$  subunit of transducin, but not to G $\alpha$  GDP- $\beta\gamma$ , *FEBS Lett.* 362, 286–290.